

# Two-loop soft anomalous dimensions with massive and massless quarks

Nikolaos Kidonakis  
 Kennesaw State University, Kennesaw, GA 30144, USA

I present results for two-loop soft anomalous dimensions, which are derived from dimensionally regularized diagrams with eikonal quark lines and control soft-gluon emission in hard-scattering processes. Detailed results for the UV poles of the eikonal integrals are shown for massive quarks, and the massless limit is also taken. The construction of soft anomalous dimensions at two-loops allows soft-gluon resummations at NNLL accuracy.

## 1. Introduction

Soft-gluon resummation formalisms for top quark production and other hard scattering cross sections beyond leading logarithms are formulated in terms of exponentials of soft anomalous dimensions that control noncollinear soft-gluon emission (see e.g. [1]). The calculations of these anomalous dimensions [2, 3] are performed using the eikonal approximation, which is valid for describing the emission of soft gluons from partons in the hard scattering. The approximation leads to a simplified form of the Feynman rules by removing the Dirac matrices from the calculation. When the gluon momentum,  $k$ , goes to zero, the Feynman rule for the quark-gluon vertex reduces to  $g_s T_F^c v^\mu / v \cdot k$  with  $v$  a dimensionless velocity vector.

Here we calculate diagrams and derive the soft anomalous dimension for top quark pair production via  $e^+e^- \rightarrow t\bar{t}$  through two loops [3]. We also discuss the massless limit and extensions to other processes.

Writing the soft anomalous dimension  $\Gamma_S$  as a series in  $\alpha_s$

$$\Gamma_S = \frac{\alpha_s}{\pi} \Gamma_S^{(1)} + \left(\frac{\alpha_s}{\pi}\right)^2 \Gamma_S^{(2)} + \dots \quad (1)$$

we calculate the one- and two-loop expressions for  $\Gamma_S$ . We use the Feynman gauge and we employ dimensional regularization with  $n = 4 - \epsilon$  dimensions. The soft anomalous dimension can be determined from the coefficients of the ultraviolet (UV) poles of the eikonal diagrams.

We do not include the color factors in the individual diagrams below, but take them into account when assembling all the pieces together in the last section. The Appendix lists some of the integrals calculated for the evaluation of the diagrams.

## 2. One-loop diagrams

In this section we calculate the one-loop diagrams in Fig. 1. We define  $\beta = \sqrt{1 - 4m^2/s}$  with  $m$  the heavy quark mass and  $s$  the squared c.m. energy. We label the two heavy quark lines by  $i$  and  $j$ . Using the

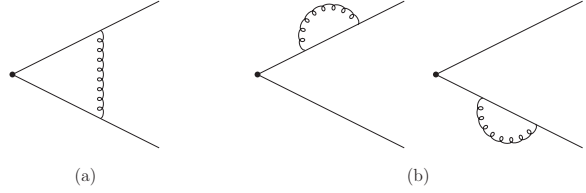


Figure 1: One-loop diagrams with heavy-quark eikonal lines.

relation  $v = p \sqrt{2/s}$ , with  $p$  the momentum, we have  $v_i^2 = v_j^2 = (1 - \beta^2)/2$  and  $v_i \cdot v_j = (1 + \beta^2)/2$ .

We begin with the integral  $I_{1a}$  for the diagram in Fig. 1(a) given by

$$I_{1a} = g_s^2 \int \frac{d^n k}{(2\pi)^n} \frac{(-i)g_{\mu\nu}}{k^2} \frac{v_i^\mu}{v_i \cdot k} \frac{(-v_j^\nu)}{(-v_j \cdot k)}. \quad (2)$$

Using Feynman parameterization and after several manipulations and separation of UV and infrared (IR) singularities, we find through Eq. (69) the UV poles

$$I_{1a} = \frac{\alpha_s}{\pi} \frac{(1 + \beta^2)}{2\beta} \frac{1}{\epsilon} \ln \left( \frac{1 - \beta}{1 + \beta} \right). \quad (3)$$

Next we calculate the one-loop self-energy diagrams in Fig. 1(b) given by

$$I_{1b} = g_s^2 \int \frac{d^n k}{(2\pi)^n} \frac{(-i)g_{\mu\nu}}{k^2} \frac{v_i^\mu}{v_i \cdot (k' - k)} \frac{v_i^\nu}{v_i \cdot k'}. \quad (4)$$

Here we have introduced the regulator  $k'$ , i.e. the external quark momentum is  $p_i + k'$ , so as to use the eikonal rules. We then expand the above expression around  $v_i \cdot k' = 0$  at constant  $\epsilon$ . The expansion gives an irrelevant  $1/v_i \cdot k'$  term, a constant term, and linear and higher-order terms in  $v_i \cdot k'$  which vanish when setting  $k' = 0$ . The remaining term is then

$$I_{1b} = \frac{i g_s^2 v_i^2}{(2\pi)^n} \int \frac{d^n k}{k^2 (v_i \cdot k)^2}. \quad (5)$$

We isolate the UV poles and using Eq. (70) we find

$$I_{1b} = \frac{\alpha_s}{\pi} \frac{1}{\epsilon}. \quad (6)$$

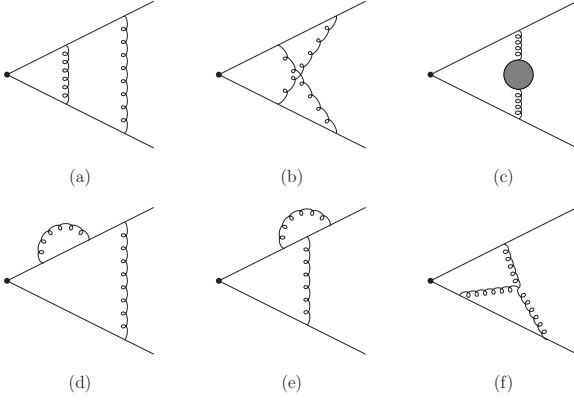


Figure 2: Two-loop vertex diagrams with heavy-quark eikonal lines.

The one-loop soft anomalous dimension is then read off the coefficient of the UV poles of the one-loop diagrams through

$$C_F[I_{1a} + I_{1b}] = -\frac{\alpha_s \Gamma_S^{(1)}}{\pi \epsilon} \quad (7)$$

which gives

$$\Gamma_S^{(1)} = C_F \left[ -\frac{(1+\beta^2)}{2\beta} \ln \left( \frac{1-\beta}{1+\beta} \right) - 1 \right] \quad (8)$$

with  $C_F = (N_c^2 - 1)/(2N_c)$  the color factor.

When expressed in terms of the cusp angle  $\gamma = \cosh^{-1} \left( v_i \cdot v_j / \sqrt{v_i^2 v_j^2} \right) = \ln[(1+\beta)/(1-\beta)]$  this becomes  $\Gamma_S^{(1)} = C_F(\gamma \coth \gamma - 1)$  and is also known as a cusp anomalous dimension [4, 5].

### 3. Two-loop vertex diagrams

The two-loop diagrams can be separated into two groups, shown in Fig. 2 and 3. The calculations are challenging due to the presence of a heavy quark mass and they involve multiple complicated integrals and delicate separations of infrared and ultraviolet poles, which by construction of the soft function are opposites of each other [2]. The analytical structure of the results involves logarithms and polylogarithms.

In this section we calculate the two-loop vertex diagrams of Fig. 2. We also have to include the one-loop counterterms to these diagrams. We will denote by  $I_2'$  the diagrams in Fig. 2 and by  $I_2^{c.t.}$  their counterterms. The total contribution will then be  $I_2 = I_2' + I_2^{c.t.}$ .

We find it convenient to define

$$M_\beta = (4 \ln 2 + \ln \pi - \gamma_E - i\pi) \ln \left( \frac{1-\beta}{1+\beta} \right)$$

$$+ \frac{1}{2} \ln^2(1+\beta) - \frac{1}{2} \ln^2(1-\beta) - \text{Li}_2 \left( \frac{1+\beta}{2} \right) + \text{Li}_2 \left( \frac{1-\beta}{2} \right). \quad (9)$$

#### 3.1. $I_{2a}$ and $I_{2b}$

In this section we calculate the integrals  $I_{2a}$  and  $I_{2b}$  for the two-loop diagrams in Figs. 2(a) and 2(b). Note that there is no counterterm for diagram 2(b), so  $I_{2b} = I_{2b}'$ .

Diagram 2(b) is given by

$$I_{2b} = g_s^4 \int \frac{d^n k_1}{(2\pi)^n} \frac{d^n k_2}{(2\pi)^n} \frac{(-i)g_{\mu\nu}}{k_1^2} \frac{(-i)g_{\rho\sigma}}{k_2^2} \times \frac{v_i^\mu}{v_i \cdot k_1} \frac{v_i^\rho}{v_i \cdot (k_1 + k_2)} \frac{(-v_j^\nu)}{-v_j \cdot (k_1 + k_2)} \frac{(-v_j^\sigma)}{-v_j \cdot k_2}. \quad (10)$$

Now, we begin with the  $k_2$  integral and use Feynman parameterization. Performing first the  $k_2$  integration and then an integration over one of the parameters, we have

$$I_{2b} = -i \frac{\alpha_s^2}{\pi^2} 2^{-4+\epsilon} \pi^{-2+3\frac{\epsilon}{2}} \Gamma \left( 1 - \frac{\epsilon}{2} \right) \Gamma(1+\epsilon) \times (1+\beta^2)^2 \int_0^1 dz \int_0^1 dy (1-y)^{-\epsilon} \times \left[ 2\beta^2(1-y)^2 z^2 - 2\beta^2(1-y)z - \frac{(1-\beta^2)}{2} \right]^{-1+\frac{\epsilon}{2}} \times \int \frac{d^n k_1}{k_1^2 v_i \cdot k_1 [(v_i - v_j)z + v_j] \cdot k_1}^{1+\epsilon}. \quad (11)$$

Next we proceed with the  $k_1$  integral

$$\int \frac{d^n k_1}{k_1^2 v_i \cdot k_1 [(v_i - v_j)z + v_j] \cdot k_1}^{1+\epsilon} = -i(-1)^{-3\frac{\epsilon}{2}} \times 2^{2+3\epsilon} \pi^{2-\frac{\epsilon}{2}} \frac{\Gamma(1+\frac{3\epsilon}{2})}{\Gamma(1+\epsilon)} \int_0^1 dx_1 x_1^{-1+2\epsilon} (1-x_1)^{-1-2\epsilon} \times \int_0^1 dx_2 (1-x_2)^\epsilon \{ [x_2 v_i + (1-x_2)((v_i - v_j)z + v_j)]^2 \}^{-1-3\frac{\epsilon}{2}}. \quad (12)$$

The integral over  $x_1$  contains both UV and IR singularities. We isolate the UV singularities via

$$\int_0^1 dx_1 x_1^{-1+2\epsilon} (1-x)^{-1-2\epsilon} = \int_0^1 dx_1 x_1^{-1+2\epsilon} + \int_0^1 dx_1 x_1^{-1+2\epsilon} [(1-x)^{-1-2\epsilon} - 1] = \frac{1}{2\epsilon} + \text{IR}. \quad (13)$$

We set  $\epsilon = 0$  in the integral over  $x_2$  since it is UV finite. We thus find the UV poles of the  $k_1$  integral

$$\int \frac{d^n k_1}{k_1^2 v_i \cdot k_1 [(v_i - v_j)z + v_j] \cdot k_1}^{1+\epsilon} = -i 2\pi^2 \frac{1}{\epsilon} \times \frac{1}{\beta(1-z)} \left[ \tanh^{-1}(\beta(1-2z)) - \tanh^{-1}(-\beta) \right]. \quad (14)$$

Using this result in the expression for  $I_{2b}$ , Eq. (11), and performing the  $y$  and  $z$  integrals, we find

$$I_{2b} = \frac{\alpha_s^2 (1 + \beta^2)^2}{\pi^2} \frac{1}{8\beta^2} \frac{1}{\epsilon} \left\{ -\frac{1}{3} \ln^3 \left( \frac{1 - \beta}{1 + \beta} \right) - \ln \left( \frac{1 - \beta}{1 + \beta} \right) \left[ \text{Li}_2 \left( \frac{(1 - \beta)^2}{(1 + \beta)^2} \right) + \zeta_2 \right] + \text{Li}_3 \left( \frac{(1 - \beta)^2}{(1 + \beta)^2} \right) - \zeta_3 \right\}. \quad (15)$$

Diagrams 2(a) and 2(b) are related through the equation  $I'_{2a} + I_{2b} = \frac{1}{2} I'_{1a}$  (where we need to keep UV poles and constant terms in  $I_{1a}$ ) from which we can calculate  $I'_{2a}$ . The one-loop counterterm to  $I_{2a}$  is

$$I_{2a}^{c.t.} = \frac{\alpha_s^2 (1 + \beta^2)^2}{\pi^2} \frac{1}{8\beta^2} \left\{ -\frac{2}{\epsilon^2} \ln^2 \left( \frac{1 - \beta}{1 + \beta} \right) - \frac{1}{\epsilon} M(\beta) \ln \left( \frac{1 - \beta}{1 + \beta} \right) \right\}. \quad (16)$$

Then we find the simple relation

$$I_{2a} + I_{2b} = \frac{\alpha_s^2 (1 + \beta^2)^2}{\pi^2} \frac{(-1)}{8\beta^2} \frac{1}{\epsilon^2} \ln^2 \left( \frac{1 - \beta}{1 + \beta} \right). \quad (17)$$

### 3.2. $I_{2c}$

In this section we calculate the integrals for the three diagrams represented by Fig. 2(c). The blob represents a quark, gluon, or ghost loop. Note that an additional diagram with a four-gluon vertex vanishes.

The quark-loop diagram is given by

$$I'_{2cq} = (-1) n_f g_s^4 \int \frac{d^n k}{(2\pi)^n} \frac{d^n l}{(2\pi)^n} \frac{v_i^\mu}{v_i \cdot k} \frac{(-v_j^\rho)}{(-v_j \cdot k)} \times \frac{(-i)g_{\mu\nu}}{k^2} \frac{(-i)g_{\rho\sigma}}{k^2} \text{Tr} \left[ -i\gamma^\nu \not{l} \not{i} (-i)\gamma^\sigma i \frac{(\not{l} - \not{k})}{(l - k)^2} \right]. \quad (18)$$

After several steps, and using Eq. (71), the final result for the UV poles of  $I'_{2cq}$  is

$$I'_{2cq} = \frac{\alpha_s^2 n_f (1 + \beta^2)}{\pi^2} \frac{1}{6\beta} \left\{ -\frac{1}{\epsilon^2} \ln \left( \frac{1 - \beta}{1 + \beta} \right) - \frac{1}{\epsilon} \left[ \frac{5}{6} \ln \left( \frac{1 - \beta}{1 + \beta} \right) + M_\beta \right] \right\} \quad (19)$$

with  $n_f$  the number of light quark flavors. The one-loop counterterm is

$$I_{2cq}^{c.t.} = \frac{\alpha_s^2 n_f (1 + \beta^2)}{\pi^2} \frac{1}{6\beta} \left\{ \frac{2}{\epsilon^2} \ln \left( \frac{1 - \beta}{1 + \beta} \right) + \frac{1}{\epsilon} M_\beta \right\}. \quad (20)$$

Then the sum  $I_{2cq} = I'_{2cq} + I_{2cq}^{c.t.}$  gives

$$I_{2cq} = \frac{\alpha_s^2 n_f (1 + \beta^2)}{\pi^2} \frac{1}{6\beta} \left[ \frac{1}{\epsilon^2} - \frac{5}{6\epsilon} \right] \ln \left( \frac{1 - \beta}{1 + \beta} \right). \quad (21)$$

Next we calculate the integral for the gluon-loop diagram given by

$$I'_{2cgl} = \frac{1}{2} g_s^4 \int \frac{d^n k}{(2\pi)^n} \frac{d^n l}{(2\pi)^n} \frac{v_i^\mu}{v_i \cdot k} \frac{(-v_j^\rho)}{(-v_j \cdot k)} \times \frac{(-i)g_{\mu\mu'}}{k^2} \frac{(-i)g_{\rho\rho'}}{l^2} \frac{(-i)g_{\sigma\sigma'}}{(k - l)^2} \frac{(-i)g_{\nu\nu'}}{k^2} \times \left[ g^{\mu'\rho}(k + l)^\sigma + g^{\rho\sigma}(k - 2l)^{\mu'} + g^{\sigma\mu'}(-2k + l)^\rho \right] \times \left[ g^{\rho'\nu'}(l + k)^{\sigma'} + g^{\nu'\sigma'}(-2k + l)^{\rho'} + g^{\sigma'\rho'}(k - 2l)^{\nu'} \right]. \quad (22)$$

Using Eq. (71) we find for the UV poles of  $I'_{2cgl}$ ,

$$I'_{2cgl} = \frac{\alpha_s^2}{\pi^2} \frac{19(1 + \beta^2)}{96\beta} \left\{ -\frac{1}{\epsilon^2} \ln \left( \frac{1 - \beta}{1 + \beta} \right) - \frac{1}{\epsilon} \left[ \frac{58}{57} \ln \left( \frac{1 - \beta}{1 + \beta} \right) + M_\beta \right] \right\}. \quad (23)$$

The one-loop counterterm is

$$I_{2cgl}^{c.t.} = \frac{\alpha_s^2}{\pi^2} \frac{19(1 + \beta^2)}{96\beta} \left\{ \frac{2}{\epsilon^2} \ln \left( \frac{1 - \beta}{1 + \beta} \right) + \frac{1}{\epsilon} M_\beta \right\}. \quad (24)$$

Then

$$I_{2cgl} = \frac{\alpha_s^2}{\pi^2} \frac{19(1 + \beta^2)}{96\beta} \left\{ \frac{1}{\epsilon^2} - \frac{58}{57\epsilon} \right\} \ln \left( \frac{1 - \beta}{1 + \beta} \right). \quad (25)$$

Last we calculate the integral for the ghost-loop diagram given by

$$I'_{2cgh} = (-1) g_s^4 \int \frac{d^n k}{(2\pi)^n} \frac{d^n l}{(2\pi)^n} \frac{v_i^\mu}{v_i \cdot k} \frac{(-v_j^\rho)}{(-v_j \cdot k)} \times \frac{i}{l^2} l^\nu \frac{i}{(l - k)^2} (l - k)^\sigma \frac{(-i)g_{\mu\nu}}{k^2} \frac{(-i)g_{\rho\sigma}}{k^2}. \quad (26)$$

Using Eq. (71), we find

$$I'_{2cgh} = \frac{\alpha_s^2 (1 + \beta^2)}{\pi^2} \frac{1}{96\beta} \left\{ -\frac{1}{\epsilon^2} \ln \left( \frac{1 - \beta}{1 + \beta} \right) - \frac{1}{\epsilon} \left[ \frac{4}{3} \ln \left( \frac{1 - \beta}{1 + \beta} \right) + M_\beta \right] \right\}. \quad (27)$$

The one-loop counterterm is

$$I_{2cgh}^{c.t.} = \frac{\alpha_s^2 (1 + \beta^2)}{\pi^2} \frac{1}{96\beta} \left\{ \frac{2}{\epsilon^2} \ln \left( \frac{1 - \beta}{1 + \beta} \right) + \frac{1}{\epsilon} M_\beta \right\}. \quad (28)$$

Then

$$I_{2cgh} = \frac{\alpha_s^2 (1 + \beta^2)}{\pi^2} \frac{1}{96\beta} \left\{ \frac{1}{\epsilon^2} - \frac{4}{3\epsilon} \right\} \ln \left( \frac{1 - \beta}{1 + \beta} \right). \quad (29)$$

The sum of the gluon and ghost loops, Eqs. (25) and (29), denoted by  $I_{2cg}$ , is then

$$I_{2cg} = \frac{\alpha_s^2}{\pi^2} \frac{5(1 + \beta^2)}{24\beta} \left[ \frac{1}{\epsilon^2} - \frac{31}{30\epsilon} \right] \ln \left( \frac{1 - \beta}{1 + \beta} \right). \quad (30)$$

### 3.3. $I_{2d}$ and $I_{2e}$

In this section we calculate the integral  $I'_{2d}$  for the diagram in Fig. 2(d) given by

$$I'_{2d} = g_s^4 \int \frac{d^n k}{(2\pi)^n} \frac{d^n l}{(2\pi)^n} \frac{(-i)g_{\mu\nu}}{k^2} \frac{(-i)g_{\rho\sigma}}{l^2} \frac{v_i^\mu}{v_i \cdot k} \times \frac{v_i^\sigma}{v_i \cdot (k-l)} \frac{v_i^\rho}{v_i \cdot k} \frac{(-v_j^\nu)}{(-v_j \cdot k)} \quad (31)$$

as well as the integral  $I'_{2e}$  for the diagram in Fig. 2(e) given by

$$I'_{2e} = g_s^4 \int \frac{d^n k}{(2\pi)^n} \frac{d^n l}{(2\pi)^n} \frac{(-i)g_{\mu\nu}}{k^2} \frac{(-i)g_{\rho\sigma}}{l^2} \frac{v_i^\sigma}{(-v_i \cdot l)} \times \frac{v_i^\mu}{v_i \cdot (k-l)} \frac{v_i^\rho}{v_i \cdot k} \frac{(-v_j^\nu)}{(-v_j \cdot k)}. \quad (32)$$

First we note that

$$I'_{2d} + I'_{2e} = \frac{g_s^4}{(2\pi)^{2n}} v_i^2 v_i \cdot v_j \int \frac{d^n k}{k^2 (v_i \cdot k)^2 v_j \cdot k} \times \int \frac{d^n l}{l^2 v_i \cdot l} = 0 \quad (33)$$

where the last integral is zero because it is odd in  $l$ . Therefore  $I'_{2d} = -I'_{2e}$  and similarly for the counterterms, and then  $I_{2d} = -I_{2e}$ . Thus we only have to calculate  $I'_{2e}$  and its counterterm. Using Eq. (72) and including the counterterm  $I_{2e}^{c.t.} = (\alpha_s^2/\pi^2)[(1 + \beta^2)/(4\beta)][2/\epsilon^2 \ln((1 - \beta)/(1 + \beta)) + M_\beta/\epsilon]$  we find

$$I_{2e} = \frac{\alpha_s^2}{\pi^2} \frac{(1 + \beta^2)}{4\beta} \left\{ \frac{1}{\epsilon^2} \ln \left( \frac{1 - \beta}{1 + \beta} \right) - \frac{1}{\epsilon} \left[ \ln \left( \frac{1 - \beta}{1 + \beta} \right) + \frac{1}{2} \ln^2 \left( \frac{1 - \beta}{1 + \beta} \right) - \frac{1}{2} \text{Li}_2 \left( \frac{(1 - \beta)^2}{(1 + \beta)^2} \right) + \ln \left( \frac{1 - \beta}{1 + \beta} \right) \ln \left( \frac{(1 + \beta)^2}{4\beta} \right) + \frac{\zeta_2}{2} \right] \right\}. \quad (34)$$

### 3.4. $I_{2f}$

In this section we calculate the three-gluon diagram in Fig. 2(f) given by

$$I'_{2f} = g_s^4 \int \frac{d^n k_1}{(2\pi)^n} \frac{d^n k_2}{(2\pi)^n} \frac{(-i)g_{\mu\mu'}}{k_1^2} \frac{(-i)g_{\nu\nu'}}{k_2^2} \frac{(-i)g_{\rho\rho'}}{(k_1 + k_2)^2} \times \frac{v_i^\mu}{v_i \cdot k_1} \frac{(-v_j^\nu)}{(-v_j \cdot k_1)} \frac{(-v_j^{\rho'})}{-v_j \cdot (k_1 + k_2)} (-i) \times \left[ g^{\mu'\nu'} (k_1 - k_2)^{\rho'} + g^{\nu'\rho'} (k_1 + 2k_2)^{\mu'} + g^{\rho'\mu'} (-2k_1 - k_2)^{\nu'} \right]. \quad (35)$$

After many steps we find

$$I_{2f} = \frac{1}{\epsilon} \left\{ \frac{(1 + \beta^2)}{12\beta} \ln^3 \left( \frac{1 - \beta}{1 + \beta} \right) \right.$$

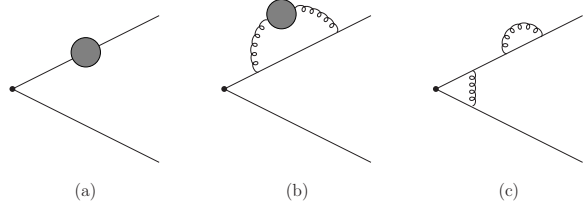


Figure 3: Two-loop heavy-quark self-energy diagrams with eikonal lines.

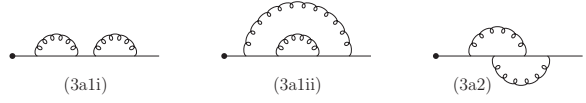


Figure 4: Detail of the diagrams of Fig. 3(a).

$$- \frac{1}{4} \left[ 2\zeta_2 + \ln^2 \left( \frac{1 - \beta}{1 + \beta} \right) \right] \times \left[ \frac{(1 + \beta^2)}{2\beta} \ln \left( \frac{1 - \beta}{1 + \beta} \right) + 1 \right] \}. \quad (36)$$

## 4. Two-loop heavy-quark self-energy diagrams

In this section we calculate the diagrams in Fig. 3 and their counterterms. We will denote by  $I'_3$  the diagrams shown in Fig. 3 and by  $I_3^{c.t.}$  their counterterms. The total contribution is then  $I_3 = I'_3 + I_3^{c.t.}$ . As for diagram 1(b) we introduce a regulator  $k'$  in the quark momentum and then expand around  $v_i \cdot k' = 0$  at constant  $\epsilon$ . We also find it convient to define

$$K_\beta = -\ln(1 - \beta^2) + 5 \ln 2 + \ln \pi - \gamma_E - i\pi. \quad (37)$$

### 4.1. $I_{3a}$

Here we calculate the three diagrams represented by Fig. 3(a) which are shown in detail in Fig. 4. Note that an additional graph involving a three-gluon vertex with all three gluons attached to the same eikonal line vanishes.

We begin with the diagram labeled (3a1i). Using Eq. (70) we find

$$I'_{3a1i} = \frac{\alpha_s^2}{\pi^2} \left\{ \frac{1}{\epsilon^2} + \frac{1}{\epsilon} K_\beta \right\} \quad (38)$$

with counterterm  $I_{3a1i}^{c.t.} = (\alpha_s^2/\pi^2)[-2/\epsilon^2 - K_\beta/\epsilon]$ . Then

$$I_{3a1i} = \frac{\alpha_s^2}{\pi^2} \frac{(-1)}{\epsilon^2}. \quad (39)$$

Next we calculate  $I'_{3a1ii}$ . Using Eq. (73) we find

$$I'_{3a1ii} = \frac{\alpha_s^2}{\pi^2} \left\{ \frac{1}{2\epsilon^2} + \frac{1}{2\epsilon} [1 + K_\beta] \right\} \quad (40)$$

with counterterm  $I_{3a1ii}^{c.t.} = (\alpha_s^2/\pi^2)[-1/\epsilon^2 - K_\beta/(2\epsilon)]$ . Then

$$I_{3a1ii} = \frac{\alpha_s^2}{\pi^2} \left\{ -\frac{1}{2\epsilon^2} + \frac{1}{2\epsilon} \right\}. \quad (41)$$

Adding Eqs. (39) and (41) and denoting the sum by  $I_{3a1}$ , we find

$$I_{3a1} = \frac{\alpha_s^2}{\pi^2} \left\{ -\frac{3}{2\epsilon^2} + \frac{1}{2\epsilon} \right\}. \quad (42)$$

Last we calculate  $I'_{3a2}$ , given by

$$I'_{3a2} = g_s^4 \int \frac{d^n k_1}{(2\pi)^n} \frac{d^n k_2}{(2\pi)^n} \frac{v_i^\mu}{v_i \cdot k'} \frac{v_i^\rho}{v_i \cdot (k' - k_1)} \\ \times \frac{v_i^\nu}{v_i \cdot (k' - k_1 - k_2)} \frac{v_i^\sigma}{v_i \cdot (k' - k_2)} \frac{(-i)g_{\mu\nu}}{k_1^2} \frac{(-i)g_{\rho\sigma}}{k_2^2}. \quad (43)$$

Using Eqs. (74), (75), and (76), we find the UV poles of the integral

$$I'_{3a2} = \frac{\alpha_s^2}{\pi^2} \left\{ -\frac{1}{\epsilon^2} - \frac{1}{\epsilon} \left[ \frac{1}{2} + K_\beta \right] \right\} \quad (44)$$

with counterterm  $I_{3a2}^{c.t.} = (\alpha_s^2/\pi^2)[2/\epsilon^2 + K_\beta/\epsilon]$ . Then

$$I_{3a2} = \frac{\alpha_s^2}{\pi^2} \left\{ \frac{1}{\epsilon^2} - \frac{1}{2\epsilon} \right\}. \quad (45)$$

## 4.2. $I_{3b}$

In this section we calculate the three self-energy diagrams (with quark, gluon, and ghost loops) represented by Fig. 3(b). Note that an additional diagram with a four-gluon vertex vanishes.

After several manipulations the quark-loop diagram becomes

$$I'_{3bq} = -4n_f \frac{g_s^4}{(2\pi)^{2n}} \frac{1}{v_i \cdot k'} \int \frac{d^n k d^n l}{k^4 v_i \cdot (k - k') l^2 (l - k)^2} \\ \times [2(v_i \cdot l)^2 - v_i^2 l^2 - 2v_i \cdot l v_i \cdot k + v_i^2 l \cdot k]. \quad (46)$$

Expanding around  $v_i \cdot k' = 0$  this gives

$$I'_{3bq} = 4n_f \frac{g_s^4}{(2\pi)^{2n}} \int \frac{d^n k}{k^4 (v_i \cdot k)^2} \int \frac{d^n l}{l^2 (l - k)^2} \\ \times [-v_i^2 l \cdot k - 2(v_i \cdot l)^2 + 2v_i \cdot l v_i \cdot k]. \quad (47)$$

A calculation of the UV poles of the integral using Eq. (77) gives

$$I'_{3bq} = \frac{\alpha_s^2 n_f}{\pi^2 3} \left\{ -\frac{1}{\epsilon^2} - \frac{1}{\epsilon} \left[ \frac{5}{6} + K_\beta \right] \right\} \quad (48)$$

with counterterm  $I_{3bq}^{c.t.} = (\alpha_s^2/\pi^2)(n_f/3)[2/\epsilon^2 + K_\beta/\epsilon]$ . Then

$$I_{3bq} = \frac{\alpha_s^2 n_f}{\pi^2 3} \left[ \frac{1}{\epsilon^2} - \frac{5}{6\epsilon} \right]. \quad (49)$$

Next we calculate the gluon-loop self-energy diagram in Fig. 3(b) which, after several manipulations, becomes

$$I'_{3bgl} = -\frac{g_s^4}{2(2\pi)^{2n}} \frac{1}{v_i \cdot k'} \int \frac{d^n k}{v_i \cdot (k - k')} \\ \times \left\{ \left[ \frac{4v_i^2}{k^2} + (n-6) \frac{(v_i \cdot k)^2}{k^4} \right] \int \frac{d^n l}{l^2 (k-l)^2} \right. \\ \left. - (4n-6) \frac{v_i \cdot k}{k^4} \int d^n l \frac{v_i \cdot l}{l^2 (k-l)^2} \right. \\ \left. + \frac{(4n-6)}{k^4} \int d^n l \frac{(v_i \cdot l)^2}{l^2 (k-l)^2} \right\}. \quad (50)$$

Expanding around  $v_i \cdot k' = 0$  this gives

$$I'_{3bgl} = -\frac{\alpha_s^2}{\pi^2} 2^{-5+2\epsilon} i \pi^{-2+\frac{3\epsilon}{2}} (1-\beta^2) \\ \times \Gamma\left(\frac{\epsilon}{2}\right) \left[ \Gamma\left(1-\frac{\epsilon}{2}\right) \right]^2 \frac{1}{\Gamma(2-\epsilon)} \\ \times \left[ 2 - \frac{(10-4\epsilon)}{8} \frac{1}{3-\epsilon} \right] \int \frac{d^n k}{(v_i \cdot k)^2 (k^2)^{1+\frac{\epsilon}{2}}}. \quad (51)$$

Using Eq. (77) the UV poles of the integral are then

$$I'_{3bgl} = \frac{\alpha_s^2 19}{\pi^2 48} \left\{ -\frac{1}{\epsilon^2} - \frac{1}{\epsilon} \left[ \frac{58}{57} + K_\beta \right] \right\}. \quad (52)$$

The counterterm is  $I_{3bgl}^{c.t.} = (\alpha_s^2/\pi^2)(19/48)[2/\epsilon^2 + K_\beta/\epsilon]$ . Then

$$I_{3bgl} = \frac{\alpha_s^2 19}{\pi^2 48} \left\{ \frac{1}{\epsilon^2} - \frac{58}{57\epsilon} \right\}. \quad (53)$$

Last we calculate the ghost-loop self-energy diagram in Fig. 3(b). After several manipulations and expanding around  $v_i \cdot k' = 0$  this gives

$$I'_{3bgh} = \frac{\alpha_s^2}{\pi^2} 2^{-6+2\epsilon} \pi^{-2+\frac{3\epsilon}{2}} i (1-\beta^2) \Gamma\left(-1+\frac{\epsilon}{2}\right) \\ \times \left[ \Gamma\left(2-\frac{\epsilon}{2}\right) \right]^2 \frac{1}{\Gamma(4-\epsilon)} \int \frac{d^n k}{(v_i \cdot k)^2 (k^2)^{1+\frac{\epsilon}{2}}}. \quad (54)$$

Using Eq. (77) the UV poles are then given by

$$I'_{3bgh} = \frac{\alpha_s^2}{\pi^2 48} \left\{ -\frac{1}{\epsilon^2} - \frac{1}{\epsilon} \left[ \frac{4}{3} + K_\beta \right] \right\} \quad (55)$$

with counterterm  $I_{3bgh}^{c.t.} = (\alpha_s^2/\pi^2)(1/48)[2/\epsilon^2 + K_\beta/\epsilon]$ . Then

$$I_{3bgh} = \frac{\alpha_s^2}{\pi^2 48} \left\{ \frac{1}{\epsilon^2} - \frac{4}{3\epsilon} \right\}. \quad (56)$$

The sum of the gluon and ghost loops, Eqs. (53) and (56), denoted by  $I_{3bg}$ , is then

$$I_{3bg} = \frac{\alpha_s^2}{\pi^2 12} \left[ \frac{1}{\epsilon^2} - \frac{31}{30\epsilon} \right]. \quad (57)$$

### 4.3. $I_{3c}$

Finally we calculate the diagram in Fig. 3(c). Using Eqs. (69) and (70) and adding the one-loop counterterm, we find

$$I_{3c} = \frac{\alpha_s^2}{\pi^2} \frac{(1+\beta^2)}{2\beta} \frac{(-1)}{\epsilon^2} \ln\left(\frac{1-\beta}{1+\beta}\right). \quad (58)$$

## 5. Two-loop soft anomalous dimension

We now combine the kinematic results from sections 3 and 4 with color and symmetry factors. The contribution of the diagrams in Figs. (2) and (3) to the two-loop soft anomalous dimension is

$$\begin{aligned} & C_F^2 [I_{2a} + I_{2b} + 2I_{2d} + 2I_{2e} + I_{3a1} + I_{3a2} + I_{3c}] \\ & + C_F C_A \left[ -\frac{1}{2}I_{2b} + I_{2f} - I_{2cg} - I_{2e} - I_{3bg} - \frac{1}{2}I_{3a2} \right] \\ & + \frac{1}{2}C_F [I_{2cq} + I_{3bq}] \\ & = \frac{\alpha_s^2}{\pi^2} \left[ -\frac{1}{2\epsilon^2} \left( \Gamma_S^{(1)} \right)^2 + \frac{\beta_0}{4\epsilon^2} \Gamma_S^{(1)} - \frac{1}{2\epsilon} \Gamma_S^{(2)} \right]. \quad (59) \end{aligned}$$

On the right-hand side of Eq. (59) in addition to  $\Gamma_S^{(2)}$ , which appears in the coefficient of the  $1/\epsilon$  pole, there also appear terms from the exponentiation of the one-loop result and the running of the coupling, with  $\beta_0 = (11/3)C_A - 2n_f/3$ ,  $C_A = N_c$ , which account for all the double poles of the graphs. From Eq. (59) we solve for the two-loop soft anomalous dimension:

$$\begin{aligned} \Gamma_S^{(2)} = & \frac{K}{2} \Gamma_S^{(1)} + C_F C_A \left\{ \frac{1}{2} + \frac{\zeta_2}{2} + \frac{1}{2} \ln^2 \left( \frac{1-\beta}{1+\beta} \right) \right. \\ & - \frac{(1+\beta^2)^2}{8\beta^2} \left[ \zeta_3 + \zeta_2 \ln \left( \frac{1-\beta}{1+\beta} \right) + \frac{1}{3} \ln^3 \left( \frac{1-\beta}{1+\beta} \right) \right. \\ & \left. \left. + \ln \left( \frac{1-\beta}{1+\beta} \right) \text{Li}_2 \left( \frac{(1-\beta)^2}{(1+\beta)^2} \right) - \text{Li}_3 \left( \frac{(1-\beta)^2}{(1+\beta)^2} \right) \right] \right. \\ & - \frac{(1+\beta^2)}{4\beta} \left[ \zeta_2 - \zeta_2 \ln \left( \frac{1-\beta}{1+\beta} \right) + \ln^2 \left( \frac{1-\beta}{1+\beta} \right) \right. \\ & \left. - \frac{1}{3} \ln^3 \left( \frac{1-\beta}{1+\beta} \right) + 2 \ln \left( \frac{1-\beta}{1+\beta} \right) \ln \left( \frac{(1+\beta)^2}{4\beta} \right) \right. \\ & \left. \left. - \text{Li}_2 \left( \frac{(1-\beta)^2}{(1+\beta)^2} \right) \right] \right\} \quad (60) \end{aligned}$$

where

$$K = C_A \left( \frac{67}{18} - \zeta_2 \right) - \frac{5n_f}{9}. \quad (61)$$

A slightly different but equivalent expression is given in Ref. [3].

In terms of the cusp angle  $\gamma$  we find

$$\Gamma_S^{(2)} = \frac{K}{2} \Gamma_S^{(1)} + C_F C_A \left\{ \frac{1}{2} + \frac{\zeta_2}{2} + \frac{\gamma^2}{2} - \frac{1}{2} \coth^2 \gamma \right.$$

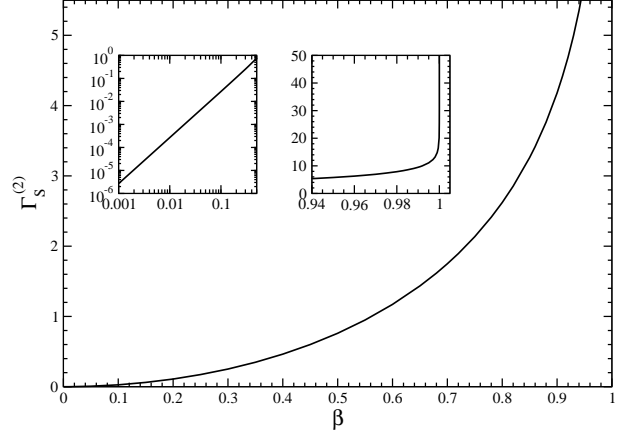


Figure 5: The two-loop soft anomalous dimension  $\Gamma_S^{(2)}$ .

$$\begin{aligned} & \times \left[ \zeta_3 - \zeta_2 \gamma - \frac{\gamma^3}{3} - \gamma \text{Li}_2(e^{-2\gamma}) - \text{Li}_3(e^{-2\gamma}) \right] \\ & - \frac{1}{2} \coth \gamma \left[ \zeta_2 + \zeta_2 \gamma + \gamma^2 + \frac{\gamma^3}{3} \right. \\ & \left. + 2\gamma \ln(1 - e^{-2\gamma}) - \text{Li}_2(e^{-2\gamma}) \right] \}. \quad (62) \end{aligned}$$

This expression is consistent with the form of the two-loop cusp anomalous dimension given in Ref. [5] (which involves a few uncalculated integrals), and it is also consistent with the two-loop heavy-quark form factor of Ref. [6].

Using the above results we can find the soft-gluon logarithms in the cross section for  $e^+e^- \rightarrow t\bar{t}$ , which are of the form  $\ln^{n-1}(\beta^2)/\beta^2$  at  $n$ -th order in  $\alpha_s$ . The first-order soft-gluon corrections are  $\sigma^{(1)} = \sigma^B (\alpha_s/\pi) 2\Gamma_S^{(1)}/\beta^2$  with  $\sigma^B$  the Born cross section. The second-order soft-gluon corrections are

$$\begin{aligned} \sigma^{(2)} = & \sigma^B \frac{\alpha_s^2}{\pi^2} \left\{ \left[ 4(\Gamma_S^{(1)})^2 - \beta_0 \Gamma_S^{(1)} \right] \frac{\ln(\beta^2)}{\beta^2} \right. \\ & \left. + \left[ 2T_1 \Gamma_S^{(1)} + 2\Gamma_S^{(2)} \right] \frac{1}{\beta^2} \right\} \quad (63) \end{aligned}$$

with  $T_1$  the NLO virtual corrections.

In Figure 5 we plot  $\Gamma_S^{(2)}$  versus  $\beta$ . The insets show the small and large  $\beta$  regions in detail. Note that both  $\Gamma_S^{(1)}$  and  $\Gamma_S^{(2)}$  vanish in the threshold limit,  $\beta = 0$ , and they both diverge in the massless limit,  $\beta = 1$ .

The small- $\beta$  expansion of Eq. (60) is

$$\begin{aligned} \Gamma_{S\text{exp}}^{(2)} = & -\frac{2}{27}\beta^2 [C_F C_A (18\zeta_2 - 47) + 5n_f C_F] \\ & + \mathcal{O}(\beta^4). \quad (64) \end{aligned}$$

$\Gamma_S^{(2)}$  is an even function of  $\beta$  and hence only even powers of  $\beta$  appear in the expansion. As shown in [3] the expansion provides a good approximation to the complete result for small  $\beta$ .

Next we study the large- $\beta$  behavior of  $\Gamma_S^{(2)}$ , Eq. (60). As  $\beta \rightarrow 1$ ,

$$\Gamma_S^{(2)} \rightarrow \frac{K}{2}\Gamma_S^{(1)} + C_F C_A \frac{(1 - \zeta_3)}{2} \quad (65)$$

with  $\Gamma_S^{(1)} = C_F \left[ \ln \left( 2v_i \cdot v_j / \sqrt{v_i^2 v_j^2} \right) - 1 \right]$ . Since  $\Gamma_S^{(1)}$  diverges at  $\beta = 1$ ,  $\Gamma_S^{(2)} \approx (K/2)\Gamma_S^{(1)}$  at that limit. This is consistent with the massless case  $\Gamma_S^{(2)} = \frac{K}{2}\Gamma_S^{(1)}$  with  $\Gamma_S^{(1)} = C_F \ln(v_i \cdot v_j)$  [7, 8, 9]. As is clear from Eq. (60) the massive case is much more complicated than the simple massless relation, and  $(K/2)\Gamma_S^{(1)}$  is just the first of many terms in the expression for  $\Gamma_S^{(2)}$ . Figure 6 shows that numerically the ratio  $(K/2)\Gamma_S^{(1)}/\Gamma_S^{(2)}$  goes to 1 as  $\beta \rightarrow 1$ , the massless limit, as expected from the above discussion, but it is significantly different from 1 at other  $\beta$  and takes the value 1.144 at the other end of the range,  $\beta = 0$ .

In the mixed massive-massless case, with  $v_i$  the heavy quark and  $v_j$  the massless quark, we find

$$\Gamma_S^{(2)} = \frac{K}{2}\Gamma_S^{(1)} + C_F C_A \frac{(1 - \zeta_3)}{4} \quad (66)$$

with

$$\Gamma_S^{(1)} = C_F \left[ \ln \left( \frac{\sqrt{2} v_i \cdot v_j}{\sqrt{v_i^2}} \right) - \frac{1}{2} \right]. \quad (67)$$

Given that the small- $\beta$  expansion gives very good approximations to  $\Gamma_S^{(2)}$  at smaller  $\beta$  while the expression  $(K/2)\Gamma_S^{(1)}$  is the large- $\beta$  limit, we can derive an approximation to  $\Gamma_S^{(2)}$ , Eq. (60), valid for all  $\beta$  using the following approximate formula:

$$\begin{aligned} \Gamma_{S \text{ approx}}^{(2)} &= \Gamma_{S \text{ exp}}^{(2)} + \frac{K}{2}\Gamma_S^{(1)} - \frac{K}{2}\Gamma_{S \text{ exp}}^{(1)} \\ &= \frac{K}{2}\Gamma_S^{(1)} + C_F C_A \left( 1 - \frac{2}{3}\zeta_2 \right) \beta^2 + \mathcal{O}(\beta^4). \end{aligned} \quad (68)$$

As seen from Fig. 6, adding just the  $\beta^2$  terms to  $(K/2)\Gamma_S^{(1)}$  provides an excellent approximation to the exact result for for all  $\beta$ . If we keep additional terms through order  $\beta^{12}$  then the approximation is extremely good and does not differ by more than one per mille anywhere in the  $\beta$  range.

Finally we discuss extensions to single top [10, 11] and top pair [10, 12] production at hadron colliders. As first shown in Ref. [3], since the two-loop soft anomalous dimensions for single top and top pair processes involve eikonal graphs with both massless and massive eikonal lines, it is clear that the simple massless relation  $\Gamma_S^{(2)} = (K/2)\Gamma_S^{(1)}$  will not hold. This observation was also made later in Refs. [13, 14]. The two-loop soft anomalous dimension  $\Gamma_S^{(2)}$  derived in [3] and in this paper is an essential ingredient for

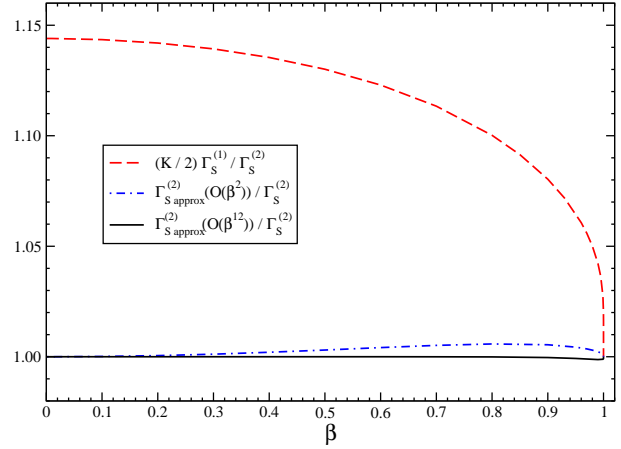


Figure 6: Approximations to  $\Gamma_S^{(2)}$ .

next-to-next-to-leading logarithm (NNLL) resummation for heavy quark hadroproduction and has been used in very recent calculations [14, 15, 16, 17].

## Acknowledgments

This work was supported by the National Science Foundation under Grant No. PHY 0855421.

## Appendix

We list results for the UV poles of several of the many integrals needed in the calculation of the two-loop soft anomalous dimension.

$$\begin{aligned} \int \frac{d^n k}{k^2 v_i \cdot k v_j \cdot k} &= \frac{i}{\epsilon} (-1)^{-1-\frac{\epsilon}{2}} \pi^{2-\frac{\epsilon}{2}} 2^{3+3\frac{\epsilon}{2}} \\ &\times \Gamma \left( 1 + \frac{\epsilon}{2} \right) {}_2F_1 \left( \frac{1}{2}, 1 + \frac{\epsilon}{2}; \frac{3}{2}; \beta^2 \right) \\ &= \frac{i4\pi^2}{\beta} \left\{ \frac{1}{\epsilon} \ln \left( \frac{1-\beta}{1+\beta} \right) \right. \\ &+ \frac{1}{2} (2 \ln 2 - \ln \pi - \gamma_E - i\pi) \ln \left( \frac{1-\beta}{1+\beta} \right) \\ &+ \frac{1}{4} \ln^2(1+\beta) - \frac{1}{4} \ln^2(1-\beta) \\ &\left. - \frac{1}{2} \text{Li}_2 \left( \frac{1+\beta}{2} \right) + \frac{1}{2} \text{Li}_2 \left( \frac{1-\beta}{2} \right) \right\} + \mathcal{O}(\epsilon) \end{aligned} \quad (69)$$

where  ${}_2F_1$  is the Gauss hypergeometric function.

$$\int \frac{d^n k}{k^2 (v_i \cdot k)^2} = \frac{i}{\epsilon} (-1)^{1-\frac{\epsilon}{2}} \pi^{2-\frac{\epsilon}{2}} 2^{3+3\frac{\epsilon}{2}}$$

$$\begin{aligned}
& \times (1 - \beta^2)^{-1 - \frac{\epsilon}{2}} \Gamma\left(1 + \frac{\epsilon}{2}\right) \\
& = -\frac{i8\pi^2}{1 - \beta^2} \left[ \frac{1}{\epsilon} - \frac{1}{2} \ln(1 - \beta^2) \right. \\
& \quad \left. + \frac{3}{2} \ln 2 - \frac{1}{2} \ln \pi - \frac{\gamma_E}{2} - \frac{i\pi}{2} \right] + \mathcal{O}(\epsilon). \quad (70)
\end{aligned}$$

$$\begin{aligned}
& \int \frac{d^n k}{(k^2)^{1 + \frac{\epsilon}{2}} v_i \cdot k v_j \cdot k} = \frac{i}{\epsilon^2} \frac{(-1)^{1 - \epsilon}}{\beta} 2^{2\epsilon} \\
& \quad \times \pi^{2 - \frac{\epsilon}{2}} \Gamma(1 + \epsilon) \frac{1}{\Gamma(1 + \frac{\epsilon}{2})} \\
& \quad \times \left[ (1 - \beta)^{-\epsilon} {}_2F_1\left(-\epsilon, 1 + \epsilon; 1 - \epsilon; \frac{1 - \beta}{2}\right) \right. \\
& \quad \left. - (1 + \beta)^{-\epsilon} {}_2F_1\left(-\epsilon, 1 + \epsilon; 1 - \epsilon; \frac{1 + \beta}{2}\right) \right]. \quad (71)
\end{aligned}$$

$$\begin{aligned}
& \int \frac{d^n k}{k^2 (v_i \cdot k)^{1 + \epsilon} v_j \cdot k} = \frac{i\pi^{2 - \frac{\epsilon}{2}}}{\epsilon(1 + \epsilon)} 2^{2 + \frac{9\epsilon}{2}} (-1)^{-1 - \frac{3\epsilon}{2}} \\
& \quad \times (1 - \beta^2)^{-1 - \frac{3\epsilon}{2}} \Gamma\left(1 + \frac{3\epsilon}{2}\right) \frac{1}{\Gamma(1 + \epsilon)} \\
& \quad \times F_1\left[1 + \epsilon; 1 + \frac{3\epsilon}{2}, 1 + \frac{3\epsilon}{2}; 2 + \epsilon; \frac{2\beta}{1 + \beta}, \frac{-2\beta}{1 - \beta}\right] \quad (72)
\end{aligned}$$

where  $F_1$  is the Appell hypergeometric function.

$$\begin{aligned}
& \int \frac{d^n k_2}{k_2^2 [v_i \cdot (k_1 + k_2)]^2} = \frac{i}{\epsilon} \frac{(-1)^{-1 + \frac{\epsilon}{2}}}{(1 + \epsilon)} 2^{4 - \frac{\epsilon}{2}} \pi^{\frac{3 - \epsilon}{2}} \\
& \quad \times (1 - \beta^2)^{-1 + \frac{\epsilon}{2}} (v_i \cdot k_1)^{-\epsilon} \Gamma\left(1 + \frac{\epsilon}{2}\right) \\
& \quad \times \Gamma\left(1 - \frac{\epsilon}{2}\right) \Gamma\left(\frac{3 + \epsilon}{2}\right). \quad (73)
\end{aligned}$$

$$\begin{aligned}
& \int \frac{d^n k}{k^2 (v_i \cdot k)^{2 + \epsilon}} = \frac{i\pi^{2 - \frac{\epsilon}{2}}}{\epsilon(1 + \epsilon)} 2^{2 + \frac{9\epsilon}{2}} (-1)^{-1 - \frac{3\epsilon}{2}} \\
& \quad \times (1 - \beta^2)^{-1 - \frac{3\epsilon}{2}} \Gamma\left(1 + \frac{3\epsilon}{2}\right) \frac{1}{\Gamma(1 + \epsilon)}. \quad (74)
\end{aligned}$$

$$\begin{aligned}
& \int \frac{d^n k_1}{k_1^2 v_i \cdot k_1 v_i \cdot (k_1 + k_2)} = \frac{i}{\epsilon} (-1)^{\frac{\epsilon}{2}} 2^{2 - \frac{\epsilon}{2}} \pi^{\frac{3 - \epsilon}{2}} \\
& \quad \times (v_i \cdot k_2)^{-\epsilon} (1 - \beta^2)^{-1 + \frac{\epsilon}{2}} \Gamma\left(1 + \frac{\epsilon}{2}\right) \\
& \quad \times \Gamma\left(1 - \frac{\epsilon}{2}\right) \Gamma\left(\frac{\epsilon - 1}{2}\right). \quad (75)
\end{aligned}$$

$$\begin{aligned}
& \int \frac{d^n k_2}{k_2^2 v_i \cdot k_2 [v_i \cdot (k_1 + k_2)]^2} = \frac{i}{1 - \epsilon} (-1)^{1 + \frac{\epsilon}{2}} \\
& \quad \times 2^{3 - \frac{3\epsilon}{2}} \pi^{2 - \frac{\epsilon}{2}} (v_i \cdot k_1)^{-1 - \epsilon} (1 - \beta^2)^{-1 + \frac{\epsilon}{2}} \\
& \quad \times \Gamma\left(1 - \frac{\epsilon}{2}\right) \Gamma(1 + \epsilon). \quad (76)
\end{aligned}$$

$$\begin{aligned}
& \int \frac{d^n k}{(k^2)^{1 + \frac{\epsilon}{2}} (v_i \cdot k)^2} = \frac{i}{\epsilon} (-1)^{-1 - \epsilon} 2^{2 + 3\epsilon} \pi^{2 - \frac{\epsilon}{2}} \\
& \quad \times (1 - \beta^2)^{-1 - \epsilon} \Gamma(1 + \epsilon) \frac{1}{\Gamma(1 + \frac{\epsilon}{2})}. \quad (77)
\end{aligned}$$

## References

- [1] N. Kidonakis, Phys. Rev. D **73**, 034001 (2006) [hep-ph/0509079]; D **77**, 053008 (2008), arXiv:0711.0142 [hep-ph]; Mod. Phys. Lett. A **19**, 405 (2004) [hep-ph/0401147].
- [2] N. Kidonakis and G. Sterman, Phys. Lett. B **387**, 867 (1996); Nucl. Phys. **B505**, 321 (1997) [hep-ph/9705234]; N. Kidonakis, G. Oderda, and G. Sterman, Nucl. Phys. **B531**, 365 (1998) [hep-ph/9803241].
- [3] N. Kidonakis, Phys. Rev. Lett. **102**, 232003 (2009), arXiv:0903.2561 [hep-ph].
- [4] S.V. Ivanov, G.P. Korchemsky, and A.V. Radyushkin, Yad. Fiz. **44**, 230 (1986) [Sov. J. Nucl. Phys. **44**, 145 (1986)].
- [5] G.P. Korchemsky, A.V. Radyushkin, Phys. Lett. B **171**, 459 (1986); Nucl. Phys. **B283**, 342 (1987); Phys. Lett. B **279**, 359 (1992) [hep-ph/9203222].
- [6] W. Bernreuther, R. Bonciani, T. Gehrmann, R. Heinesch, T. Leineweber, P. Mastrolia, and E. Remiddi, Nucl. Phys. **B706**, 245 (2005) [hep-ph/0406046].
- [7] S.M. Aybat, L.J. Dixon, and G. Sterman, Phys. Rev. D **74**, 074004 (2006) [hep-ph/0607309].
- [8] T. Becher and M. Neubert, Phys. Rev. Lett. **102**, 162001 (2009), arXiv:0901.0722 [hep-ph].
- [9] E. Gardi and L. Magnea, JHEP **03**, 079 (2009), arXiv:0901.1091 [hep-ph].
- [10] N. Kidonakis, in these proceedings, arXiv:0909.0037 [hep-ph].
- [11] N. Kidonakis, Phys. Rev. D **74**, 114012 (2006) [hep-ph/0609287]; Phys. Rev. D **75**, 071501 (2007) [hep-ph/0701080].
- [12] N. Kidonakis and R. Vogt, Phys. Rev. D **68**, 114014 (2003) [hep-ph/0308222]; Phys. Rev. D **78**, 074005 (2008), arXiv:0805.3844 [hep-ph].
- [13] A. Mitov, G. Sterman, and I. Sung, Phys. Rev. D **79**, 094015 (2009), arXiv:0903.3241 [hep-ph].
- [14] T. Becher and M. Neubert, Phys. Rev. D **79**, 125004 (2009), arXiv:0904.1021 [hep-ph].
- [15] M. Beneke, P. Falgari, and C. Schwinn, arXiv:0907.1443 [hep-ph].
- [16] M. Czakon, A. Mitov, and G. Sterman, arXiv:0907.1790 [hep-ph].
- [17] A. Ferroglia, M. Neubert, B.D. Pecjak, and L.L. Yang, arXiv:0907.4791 [hep-ph]; arXiv:0908.3676 [hep-ph].